BIO-OIL AND BIO-CRUDE GASIFICATION FOR SYNGAS PRODUCTION: ENERGY, EXERGY AND ENVIRONMENTAL ANALYSES

Ana Buelvas,[1]
Universidad del Norte
UREMA Research Unit, Department of Mechanical Engineering, Barranquilla 080001, Colombia
buelvasana@uninorte.edu.co
ASME Membership: 21100060843

Daniel A. Quintero - Coronel
Universidad del Norte
UREMA Research Unit, Department of Mechanical Engineering, Barranquilla 080001, Colombia
quinteroda@uninorte.edu.co

[2]**Juan Fajardo**
Universidad Tecnológica de Bolívar
EOLITO Research Unit, Faculty Engineering, Cartagena 130001, Colombia
jfajardo@utb.edu.co

Deibys Barreto
Universidad Tecnológica de Bolívar
EOLITO Research Unit, Faculty Engineering, Cartagena 130001, Colombia
dbarreto@utb.edu.co

Antonio Bula
Universidad del Norte
UREMA Research Unit, Department of Mechanical Engineering, Barranquilla 080001, Colombia
abula@uninorte.edu.co
ASME ID: 5904842

Arturo González- Quiroga
Universidad del Norte
UREMA Research Unit, Department of Mechanical Engineering, Barranquilla 080001, Colombia
arturoq@uninorte.edu.co

[2] *Corresponding author: Juan Fajardo*
Email: jfajardo@utb.edu.co

ABSTRACT

This study investigates the thermodynamic and environmental performance of indirect biomass gasification pathways based on fast pyrolysis products. A simulation framework was developed in Aspen Plus® integrating the Ranzi kinetic mechanism to model the conversion of bio-oil and bio-crude, considering both air and steam as gasifying agents. The environmental performance was evaluated using the Waste Reduction Algorithm.

The results reveal a clear trade-off between energy efficiency and exergy performance depending on the gasification medium. Air-based gasification achieves higher energy efficiencies, while steam-based configurations enhance exergy performance due to increased hydrogen production in the syngas. Among the evaluated feedstocks, oil palm empty fruit bunches (EFB) show superior thermodynamic performance compared to rice husk (RH), which is mainly limited by its higher ash content.

For EFB, the highest energy efficiency reaches 54.5% under air gasification, while steam operation improves exergy efficiency up to 70.1%. In contrast, RH presents lower efficiency values, ranging from approximately 43% in energy efficiency and up to 64% in exergy efficiency depending on the operating conditions. Similar trends are observed for bio-crude gasification, although with slightly lower energy efficiencies due to increased thermal requirements.

From an environmental perspective, higher potential environmental impact (PEI) values are associated with rice husk, particularly under steam conditions, due to additional emissions linked to ash-related processes. Despite this, the overall environmental indicators remain within acceptable ranges compared to similar studies.

These findings demonstrate that indirect gasification routes based on bio-oil and bio-crude constitute a promising alternative to conventional biomass gasification, offering improved exergy performance and competitive environmental outcomes. The results provide relevant insights for the design and optimization of sustainable biorefinery systems.

1. INTRODUCTION

To fight climate change, we need to curb our consumption of fossil fuels. For the chemical and plastic industries, it is mandatory to find alternative carbon sources to shift towards more sustainable, climate-friendly production and consumption. Renewable carbon comprises all carbon sources that avoid or substitute for the use of additional fossil carbon from the geosphere [1], [2]. The focus here is on residual lignocellulosic biomass (RLB), a ubiquitous source of biogenic carbon. Biogenic carbon refers to carbon that is part of the natural carbon cycle, or short-cycle carbon, according to the IPCC, originating from contemporary biological processes such as photosynthesis [2]. In this case, RLB is first transformed via fast pyrolysis into bio-oil, biochar, and non-condensable gases [3]. Pyrolysis oil or a mixture of pyrolysis oil and pulverized biochar (bio-crude) can then be gasified into syngas, the starting point to produce high-value chemicals and fuels [4] [5]. Here, we use energy, exergy, and environmental analyses to compare these alternatives.

Biomass gasification has been widely identified as a viable route for generating gases with low to medium heating values [6], [7]. In recent years, research efforts have focused on improving the design and performance of gasification systems from a process engineering perspective. For example, Ishaq et al. [8] proposed an integrated configuration that combines biomass gasification with thermoelectric-based multigeneration systems, aiming to enhance process sustainability. Similarly, Zhang et al. [9] developed an autothermal gasification approach based on CaO looping to improve overall energy efficiency. In another study, Wu et al. [10] introduced a hybrid gasification

system using a steam–air mixture coupled with solar energy, integrating cooling, heating, and power production. Their findings indicate that such combined systems can effectively utilize both solar resources and biomass availability within specific regions

An alternative to the direct biomass gasification route is the indirect method. The indirect method uses fast pyrolysis to produce additional biomass-derived products, such as bio-oil, biochar, and non-condensable gases [11]. Li et al. [12] demonstrated that a two-stage bio-oil gasification process is more economical than conventional biomass gasification. Their study evaluated the economic feasibility of an integrated production pathway combining fast pyrolysis and bio-oil gasification and compared it with the biomass gasification assessment conducted by Swanson et al. [13]. Similarly, Zheng et al. [14] studied, *via* experiments, the effect of air and low-temperature steam as the gasification agents on the bio-oil gasification performance. The authors observed that the H_2 concentration using air and steam was higher than that for bio-oil air gasification. In addition, bio-oil can also be blended with other energy sources to exploit its energy properties. For instance, Feng et al. [15] assessed the behavior of three bio-oil samples blended with coal/char. The authors investigated the combustion of these mixtures and observed synergy between bio-oil and coal/char, demonstrating bio-oil's versatility as a viable energy resource.

Evaluating both direct and indirect biomass gasification pathways provides valuable insight into their respective benefits and limitations. In this context, the present work employs process simulation tools to analyze different gasification scenarios involving biomass, bio-oil, and bio-crude, considering air and steam as gasifying agents.

Moreover, a comprehensive assessment is performed to compare the technical performance and environmental implications of these routes for syngas production from oil palm residues and rice husk (RH), applying the Waste Reduction Algorithm (WAR) [16]. Several methodologies have been reported in the literature to quantify environmental impacts, among which the Tool for the Reduction and Assessment of Chemical and Other Environmental Impacts (TRACI) [17], the Waste Reduction Algorithm (WAR) [18], and Life Cycle Assessment (LCA) [19] are the most widely used.

In this work, the fast pyrolysis process is modeled by coupling Aspen Plus® with an external computational routine developed by the authors, which is based on the Ranzi kinetic mechanism. This framework provides a detailed representation of biomass thermal decomposition and oxidation, incorporating 53 chemical species and 29 reactions across solid, liquid, and gaseous phases [20].

The Ranzi mechanism is employed to predict the formation and composition of bio-oil, biochar, and non-condensable gases, which are subsequently used as input streams in the Aspen Plus® simulation environment. Since certain compounds defined in the kinetic scheme are not available in the Aspen Plus® database, their thermophysical properties are estimated using the correlations reported by Gorensek et al. [21], ensuring consistency in the simulation of the biomass conversion process.

Bio-oil, with a higher density and energy content than solid biomass, offers improved transport and storage capabilities. This enables a flexible biomass supply for centralized syngas production, decoupling biomass supply and syngas demand [22]. However, if only bio-oil is used for gasification, about one-third of the biogenic carbon in

the original biomass would remain inaccessible for syngas production. Therefore, pulverized biochar can be mixed with biooil to form a dense slurry or bio-crude [23]. Bio-crude is a promising carbon carrier among other alternatives, such as pure bio-oil, charcoal, and (torrefied) pellets [2]. With a density of about 1200 kg/m^3 and an HHV of 18 to 25 GJ/m^3, bio-crude has one-half to two-thirds the volumetric energy density of heating oil (HHV 36 GJ/m^3) [4]. Among the processing advantages of bio-oil and bio-crude gasification are almost complete carbon conversion, high gasification pressure, and almost tar-free syngas [4].

A review by [23] summarizes bio-crude preparation technology and compares it with conventional coal slurry technology, highlighting the simplicity of the bio-crude preparation process. This work also discusses the effects of biochar particle size, loading level, and adsorption capacity, as well as the addition of other chemicals such as methanol and glycerol. As highlighted by Henrich et al. [24], bio-crude can be pumped into a slagging entrained-flow gasifier, atomized, and converted to syngas at high pressure and temperature.

Pressurized bed gasifiers produce an almost tar-free syngas by providing high gasification temperatures and pressures. This gasifier outlet condition simplifies downstream gas purification processes and eliminates the need for intermediate compression before synthesis. Syngas could be supplemented with low-emissions hydrogen and then used to produce chemical products such as synthetic natural gas and methanol[25] [26]. Steam gasification is quite promising in this context for reducing the

required external hydrogen, if carbon conversion (mainly to CO, but also to CO_2 and CH_4) is almost complete.

Recent studies have further expanded the understanding of biomass-derived feedstocks and their thermochemical conversion into syngas, highlighting both technological advancements and integration opportunities [27]. These contributions emphasize the optimization of gasification systems and improvements in process efficiency [28], as well as the exploration of hybrid and multi-stage conversion routes involving intermediate products such as bio-oil and biochar [29]. In particular, prior works have addressed modeling and simulation approaches, experimental analyses of gasification performance, and the evaluation of process variables affecting syngas composition and yield [30]. Additionally, increasing attention has been given to integrated systems that enhance carbon utilization and energy efficiency, as well as to the coupling of pyrolysis and gasification stages to improve the overall sustainability of biomass valorization pathways [31]. Collectively, these studies demonstrate the growing interest in developing flexible and efficient thermochemical routes for renewable syngas production and underline the need for comprehensive assessments that combine technical, thermodynamic, and environmental criteria.

In addition to the thermodynamic evaluation, this study provides a detailed characterization of exergy flows, irreversibility sources, unit performance, and environmental impacts, which are classified into toxicological and atmospheric categories. This integrated perspective enables a more comprehensive understanding of

process behavior and supports the identification of potential improvement strategies from both thermodynamic and environmental viewpoints.

A key contribution of this work is the application of the Waste Reduction Algorithm to assess the environmental performance of syngas production from rice husk and oil palm empty fruit bunches. Furthermore, the simultaneous use of process simulation with both environmental and exergy analyses offer a robust framework for evaluating and comparing alternative designs based on sustainable biomass resources.

The structure of the paper is as follows. Section 2 outlines the gasification routes analyzed and describes the methodological approach for the exergy and environmental assessments. Section 3 discusses the main findings and their implications, while Section 4 summarizes the conclusions and highlights directions for future research.

2. MATERIALS AND METHODS

2.1 Selected feedstock

The biomass feedstocks considered in this study are rice husk (RH) and oil palm empty fruit bunches (EFB). Their physicochemical characteristics, including ultimate, proximate, and sulfur analyses, as well as their energy content, are summarized in Table 1. Within Aspen Plus®, these materials are treated as non-conventional components, requiring the definition of specific analyses ULTANAL, PROXANAL, and SULFANAL to properly estimate their thermodynamic properties for simulation purposes.

For the simulation setup, Aspen Plus® requires that both ultimate and proximate analyses be provided on a dry basis. Additionally, the moisture content of the biomass is

incorporated as an input parameter to account for its effect on the drying stage within the fast pyrolysis process.

2.2 Fast pyrolysis process, bio-oil and bio-crude gasification simulations

The process simulation is structured into several sequential stages, including feedstock preparation, drying, pyrolysis, phase separation, combustion of by-products, and final gasification of bio-oil or bio-crude. The composition of bio-oil used as input data in Aspen Plus® is derived from the Ranzi kinetic model. A schematic representation of the overall indirect gasification pathway is shown in Figure 1.

Initially, the biomass undergoes a size reduction step to meet the particle size requirements for fast pyrolysis, typically below 3 mm [32]. This operation is modeled through a crushing and screening system. The subsequent drying stage is implemented using an RStoic reactor, coupled with a calculator block that adjusts moisture removal based on the initial water content of the feedstock.

The thermal decomposition of biomass takes place in the pyrolysis section under oxygen-free conditions, producing bio-oil, biochar, and non-condensable gases [32]. This stage is represented by two Ryield reactors. The first reactor converts the non-conventional biomass into conventional components such as C, H_2, N_2, O_2, Cl, S, ash, and H_2O, enabling their treatment within Aspen Plus®. The second reactor incorporates the product distribution predicted by the Ranzi model through an external computational routine, defining the yields of bio-oil, biochar, and gaseous species [20].

Following pyrolysis, a quenching system separates the condensable and non-condensable fractions, identified as bio-oil–water mixtures and NCG streams,

respectively. This section can be conceptually associated with equipment such as flash separators or knockout drums and includes two aqueous streams corresponding to different cooling conditions [33].

Part of the biochar produced is directed to a combustion stage to supply the heat required by the pyrolysis process. In this section, the biochar is decomposed into elemental species using a Ryield reactor, and the resulting mixture is combusted in an RGibbs reactor operating with air. A design specification block determines the air flow rate needed to satisfy the thermal demand. Depending on the feedstock characteristics, a fraction of the biochar may remain unconverted and can be considered for alternative applications such as soil amendment or energy storage 34], [35] [36].

The heat generated from biochar and non-condensable gas combustion is integrated into a heat balance block, which ensures that the energy requirements of the drying and pyrolysis stages are met under adiabatic conditions. The pyrolysis temperature is set at 480 °C. The combustion of NCG is also modeled using an RGibbs reactor with controlled air input to achieve complete conversion.

Finally, the gasification stage converts bio-oil or bio-crude into syngas using either air or steam as the gasifying medium. This step is simulated using an RGibbs reactor, where the product gas mixture consists mainly of CO, CO_2, H_2, CH_4, N_2, H_2O, and O_2. For air gasification, the process is evaluated by varying the equivalence ratio (Φ) between 0.2 and 0.9, while in steam gasification scenarios, the analysis is based on different steam-to-bio-oil ratios.

2.3 Energy and exergy analysis

Aspen Plus® was employed to determine the energy requirements associated with the fast pyrolysis process and the subsequent gasification of bio-oil or bio-crude. In addition, the physical exergy values of the process streams were directly obtained from the simulation results. However, the estimation of chemical exergy required the implementation of complementary calculation approaches due to its dependence on specific thermodynamic properties.

Equations 1 and 2 show the energy and exergy balances. In these equations, the subscripts in and out representing inlet and outlet, respectively. Equations 3 show $\dot{X}$ total exergy. The exergy includes physical ($\dot{X}_{ph}$) and chemical ($\dot{X}_{ch}$) components, estimated via Equations 4 and 5, respectively.

$$\sum \dot{E}_{in} = \sum \dot{E}_{out} \tag{1}$$

$$\sum \dot{X}_{in} = \sum \dot{X}_{out} + \sum \dot{X}_{dest} \tag{2}$$

$$\dot{X} = \dot{X}_{ph} + \dot{X}_{ch} \tag{3}$$

$$\dot{X}_{ph} = \dot{m}[h - h_0 - T_0(s - s_0)] \tag{4}$$

$$\dot{X}_{ch} = \dot{n} \sum x_i(x_i^{ch} + RT_0 ln x_i) \tag{5}$$

The terms h and s represent specific enthalpy and entropy, respectively, while h_0, T_0, and s_0 denote enthalpy, temperature, and entropy in the dead state (298.15 K and 101.325 kPa). Similarly, x_i indicates the molar fraction of component i, $\dot{n}$ is the molar flow rate, R corresponds to the universal gas constant, and x_i^{ch} is the standard chemical exergy

of component i. The x_i^{ch} estimation of the compounds evaluated in this study followed a similar procedure to that reported by Peters et al. [37]. For known components, the standard chemical exergy was obtained from references [38][39]. For solids streams such as biomass and biochar, the x_i^{ch} calculation used Equation 6 [40]. In this equation, the subscript sol could indicate biomass or biochar as corresponding. Here, HHV is in kJ/kg.

$$x_i^{ch}{}_{sol} = 1.047 \cdot HHV(\tag{6}$$

On the other hand, for compounds with known Gibbs energy of formation ($\bar{g}$), their x_i^{ch} calculation used the change of the Gibbs energy defined in Equation 7.

$$x_i^{ch} = -\Delta G + \sum_{prod} x_i \left(x_i^{ch}{}_{prod}\right) - \sum_{prod} x_i (x_i^{ch}{}_{react}) \tag{7}$$

Here, ΔG is the change in Gibbs energy and subscripts $prod$ and $react$, mean products and reactive, respectively. Finally, in streams where biochar leaves the process at temperatures higher than 25°C, the physical exergy was estimated based on Equation 8 [37].

$$\dot{X}_{ph}{}_{biochar} = \dot{m} \cdot Cp_{biochar} \cdot \left[(T - T_0) - T_0 \cdot \ln\left(\frac{T}{T_0}\right)\right] \tag{8}$$

In Equation 8, $\dot{X}_{ph}{}_{biochar}$ denotes the physical exergy of biochar (kW), with the $Cp_{biochar}$ representing the specific heat capacity of the biochar using the correlation derived from data reported by Gunnar [41] for temperatures between 273 K and 1273 K. Equation 9 is a correlation for the estimation of $Cp_{biochar}$.

Equation 10 was used to calculate energy efficiency in this study. Equation 11 shows the variables to calculate the exergy efficiency (η_{Ex}). Exergy efficiency represents the exergy gained ($\dot{E}x_{gained}$) by streams of syngas and biochar.

$$\eta_t = \frac{\dot{E}_{reached}}{\dot{E}_{in}} \quad (9)$$

$$\eta_{Ex} = \frac{\dot{E}x_{gained}}{\dot{E}x_{in}} \quad (10)$$

2.4 Environmental Assessment

The environmental assessment of the evaluated gasification routes was carried out using the Waste Reduction Algorithm (WAR). This approach allows the estimation of environmental impacts in chemical processes based on key parameters such as mass flow rates, stream compositions, and energy requirements [42]. Within this framework, the concept of potential environmental impact (PEI) is introduced as an indicator to quantify the possible effects of emissions or accidental releases on surrounding ecosystems [43].

Two main perspectives are considered when evaluating PEI: the impact associated with process outputs and the impact generated within the system. The total PEI leaving the system provides a basis for comparing different process alternatives in terms of their environmental burden on external surroundings and is also useful for assessing the suitability of a given location for plant installation [44]. In contrast, the PEI generation rate reflects the net impact produced by the process itself, allowing the identification of whether the transformation pathways result in products that are harmful than the original feedstock [42], [45].

PEI out is defined by Equation 12. Here $i_{out}^{(cp)}$, $i_{out}^{(ep)}$, $i_{we}^{(ep)}$, and $i_{we}^{(cp)}$ are the rate of PEI leaving the system due to chemical interactions, the rate of PEI out of the system due to energy generation processes, and the rate of PEI out of the system as a result of the release of waste energy due to energy generation and chemical processes, respectively [18][46][47].

$$i_{out}^{(t)} = i_{out}^{(cp)} + i_{out}^{(ep)} + i_{we}^{(cp)} + i_{we}^{(ep)} \quad (11)$$

PEI generated is defined by Equation 13, where $i_{in}^{(cp)}$ and $i_{in}^{(ep)}$ are the input rate of PEI to the chemical process and the energy generation process, respectively.

$$i_{gen}^{(t)} = i_{out}^{(ep)} - i_{in}^{(cp)} + i_{out}^{(ep)} - i_{in}^{(ep)} + i_{we}^{(cp)} + i_{we}^{(ep)} \quad (12)$$

The analysis considers eight distinct environmental impact categories, which are grouped into two main classifications: toxicological and atmospheric effects. The toxicological group includes indicators such as human toxicity by ingestion (HTPI), human toxicity through dermal exposure (HTPE), aquatic toxicity potential (ATP), and terrestrial toxicity potential (TTP).

The atmospheric category comprises indicators related to air emissions and global environmental effects, including Global Warming Potential (GWP), Ozone Depletion Potential (ODP), Photochemical Oxidation Potential (PCOP), and Acidification Potential (AP).

3. RESULTS AND DISCUSSION

The process simulation was carried out in Aspen Plus® by defining the operating conditions described in Section 2 together with the chemical composition of the selected feedstocks, allowing the determination of the corresponding mass and energy balances. The composition of the products generated during fast pyrolysis, including non-condensable gases, bio-oil, biochar, and water fractions, was obtained from the model previously reported by Buelvas et al. [22].

3.1 Energy and exergy analysis

This section summarizes the key findings from the energy and exergy evaluations, which are represented through Sankey and Grassmann diagrams under a selected equivalence ratio.

3.1.1 Bio-oil gasification

For air gasification, the CO and H_2 values obtained in this study (15.69% and 2.2% for rice husk, respectively) are similar to the CO reported by Zheng et al**.** [48] (15.4%) but show a notable decrease in the H_2 content (30.69% in Zheng et al.). This may be due to the lower operating temperature (628.7 °C vs. 1000 °C), which reduces the reforming reaction rate and favors the formation of CO_2 (28.8% vs. 8%). On the other hand, in steam gasification, the simulated results show a significant increase in the H_2 fraction (43.3% for rice husk), in line with that reported by Guo et al. [49] (62.1%), although with differences attributable to the lower steam/bio-oil ratio (0.25 vs. 0.5) and the use of different raw materials. These results underscore the process's sensitivity to temperature, the oxidizing

agent, and the type of biomass used, and the role of its work in optimizing operating conditions to maximize fuel gas production.

Fig 3a and 3b show the Sankey diagram for the fast pyrolysis simulation of EFB biomass, with bio-oil gasification using air and steam as gasification agents. The bio-oil gasification with air used an equivalence ratio (Φ) of 0.25. Steam-based gasification used a steam-to-bio-oil ratio (S/B) of 0.25. Fig 3c and 3d show the Grassmann diagrams for the same cases described in Fig 3a and 3b. Exergy assessment does not consider exergy associated with macroscopic kinetic and potential energy changes.

For Fig 3a, the energy efficiency is 54.5%, while for Fig 3b, it is 49.8%. Exergy efficiency reached 64.1 and 70.1% for the cases described in Figs 3c and 3d, respectively. Although the stream Flue gas NCG contains an exploitable exergy, this was not considered in this study. Future studies could explore options to exploit this stream, which amounts to 5.3% and 4.7% of the exergy for cases described in Figs 3c and 3d, respectively.

On the other hand, Figs 4a and 4b show the Sankey diagram for the fast pyrolysis simulation of biomass from RH, with bio-oil gasification using air and steam as gasification agents. Like EFB biomass, the air and steam gasification used a Φ of 0.25 and an S/B of 0.25. The energy efficiencies for the cases described in these Figs were 43.0% and 37.6% for air and steam as gasification agents, respectively. These values were 21% and 24% lower than those reported for EFB under the same operating conditions. This difference may be due to the high ash content of rice husk, which affects the biomass's energy content.

The lower efficiencies obtained for rice husk are strongly associated with its elevated ash fraction, which reduces the effective combustible content and increases the thermal energy required to heat inert mineral matter that does not contribute to syngas production.

Similarly, the stream flue gas NCG was about 13.8% and 13.6% for air and steam as gasification agents, respectively, lower than for the same cases evaluated for EFB. Figs 4c and 5d depict the Grassmann diagrams for the same cases tried in Figs 4a and 4b. As in the simulations for EFB, the calculated efficiency represents the exergy gained by the syngas and biochar streams in Figs 4a and 4b, which amounted to 54.4% and 62.5%, respectively.

A clear trade-off is observed between energy and exergy efficiencies depending on the gasification agent. Air based gasification consistently exhibits higher energy efficiencies, while steam based gasification leads to superior exergy performance.

The higher energy efficiencies obtained with air can be attributed to its autothermal nature, in which partial oxidation reactions provide the heat required to sustain the gasification process. This reduces the need for external energy input, resulting in lower overall energy consumption. In contrast, steam gasification is an endothermic process that requires additional heat supply, which negatively affects the overall energy efficiency.

However, from an exergy perspective, steam gasification significantly enhances thermodynamic performance. This improvement is primarily due to the increased production of hydrogen through steam reforming and water gas shift reactions. Hydrogen

rich syngas has a higher chemical exergy content, which explains the increase in exergy efficiency despite the higher energy input required. Therefore, steam gasification promotes a more effective conversion of available energy into useful chemical work.

3.1.2 Bio-crude gasification

To provide an additional comparison of products obtained from the fast pyrolysis simulation, this study considered bio-crude gasification using air and steam as the gasification agents. Bio-crude is the mixture of bio-oil and biochar obtained in the fast pyrolysis process.

In the simulation, all biochar formed in EFB biomass was used to produce bio-crude. On the contrary, simulations using RH required a portion of the biochar to meet the thermal demand of the fast pyrolysis process. Therefore, the non-required biochar was mixed with bio-oil to form bio-crude in simulations using RH.

The bio-crude gasification with air as the gasification agent used an equivalence ratio of 0.25, while the steam gasification used a steam-to-bio-oil ratio of 0.25. In addition, Figs 5c and 5d display the Grassmann diagrams for these conditions. Compared with bio-oil gasification cases, the energy efficiencies achieved in bio-crude gasification for EFB are 50.7% and 44.3%, which are 6.8% and 11% lower than those for bio-oil gasification with air and steam as the gasification agents, respectively. In addition, an increase in heat losses is evident, amounting to 15.2% and 17.0%, or 8.1% and 9.8% higher than those for bio-oil gasification using air and steam, respectively. The increase in heat losses observed during bio-crude gasification is mainly associated with the additional thermal demand required for the conversion of biochar particles suspended in the slurry. Unlike volatile

bio-oil compounds, biochar undergoes slower heterogeneous gasification reactions, which intensify thermal irreversibilities and increase the fraction of energy dissipated as sensible heat rather than converted into chemical energy in the syngas.

Figs 5c and 5d depict the Grassmann diagrams for the same cases tried in Figs 5a and 5b. The exergy efficiencies obtained in the bio-crude gasification are 62.89% and 71.93% for air and steam, respectively, as the gasification agents. A 1.9% reduction was observed for bio-crude gasification with air, while the case with steam increased by 2.5%. Although the exergy efficiency is similar to that for bio-oil gasification, more energy input is necessary for bio-crude gasification.

Furthermore, Figs 6a and 6b depict the Sankey diagrams for RH fast pyrolysis simulation and bio-crude gasification using air and steam as gasification agents, while Figs 8c and 8c correspond with the Grassmann diagrams for the same conditions. Figs 6a and 6b show that the energy efficiencies reached 41.13 and 37.66% for air and steam as the gasification agents, respectively. The values are similar to those observed in bio-oil gasification cases. The principal difference occurred in the syngas temperature for air as the gasification agents, which reached 801.59 °C, 17.4% higher than the bio-oil gasification at the same Φ value. This result reveals more energy input is necessary to complete the bio-crude gasification process.

The exergy efficiencies obtained in the bio-crude gasification are 53.94% and 64.06% for air and steam, respectively, as the gasification agents. The gained exergy was associated with the syngas stream. These values are similar to those reached in bio-oil gasification, independently of the gasification agent. For example, bio-crude gasification

with air yields an exergy efficiency of 0.85%, compared with bio-oil, while bio-crude gasification with steam as the gasification agent yields an exergy efficiency 2.4% higher. However, as was mentioned, bio-crude gasification demands more energy, increasing the flow of air and steam.

Steam gasification is the most important route for utilizing bio-crude, especially when supplemented with low-emissions hydrogen to produce synthetic natural gas, methanol, and other Power - to - X products. Producing hydrogen-rich syngas by bio-crude steam gasification is a current research hotspot, and the means of regulation include changing the type of gasification agent, temperature, pressure, and using different catalysts. It is challenging to design industrial gasification facilities due to the complexity of the slurry system, and the development of simulation modeling methods offers hope for advancing bio-crude development.

When comparing bio-oil and bio-crude gasification, a reduction in energy efficiency is observed for bio-crude cases, accompanied by comparable or slightly higher exergy efficiencies, particularly under steam gasification conditions. This behavior can be explained by the presence of biochar in bio-crude. Unlike the lighter and more reactive compounds present in bio-oil, biochar undergoes slower heterogeneous reactions that require higher temperatures and longer residence times. As a result, additional thermal energy is needed to achieve complete conversion, increasing overall energy consumption and reducing energy efficiency.

From an exergy standpoint, however, the incorporation of biochar contributes to a more complete utilization of the carbon content in the original biomass. This enhances the chemical exergy of the produced syngas, particularly when steam is used, as the additional carbon in reforming reactions that generate hydrogen rich gas. Consequently, bio-crude gasification can achieve competitive or even superior exergy efficiencies despite its higher energy demand.

Overall, the results highlight a fundamental trade-off between energy efficiency and exergy performance across the evaluated scenarios. While air gasification minimizes energy requirements, steam gasification maximizes the quality and usefulness of the produced syngas. These findings suggest that process optimization should not be based solely on energy efficiency but must also consider exergy metrics, particularly in applications where syngas quality is critical, such as hydrogen or synthetic fuel production. Additionally, feedstock selection plays a crucial role, as biomass with high ash content can significantly deteriorate process performance due to increased irreversibilities and reduced effective energy conversion.

3.2 Environmental analysis

The environmental performance of the processes modeled in Aspen Plus® is analyzed in the following section.

3.2.1 Bio-oil gasification

The environmental assessment began with the estimation of both the output and generation rates of potential environmental impact (PEI). Four operating scenarios were considered to evaluate the influence of feedstock type and gasifying agent: EFB and RH,

each analyzed under air and steam conditions. The corresponding results are summarized in Table 2.

The analysis reveals that the highest PEI output rates are associated with the use of rice husk as feedstock, reaching values of 86.53 PEI/h for air gasification and 61.16 PEI/h for steam-based operation. This behavior is mainly linked to the requirement of utilizing a portion of the produced biochar to supply thermal energy within the process, which involves combustion stages that generate flue gases and ash residues, thereby increasing the overall environmental burden.

Although the air-driven configuration with rice husk exhibits the largest PEI rate on a mass basis, the steam-based scenario shows a more significant impact when normalized per unit of product. In this case, the PEI output reaches 0.136 PEI/kg, indicating that each kilogram of syngas and biochar produced is associated with a relatively higher environmental load.

Regarding the internal generation of PEI, all evaluated scenarios show comparable trends, although differences can be observed depending on the operating conditions. In particular, the EFB case with steam gasification presents the highest values, reaching 24.14 PEI/h and 0.048 PEI/kg. This indicates that, under these conditions, the process contributes more significantly to the formation of environmentally harmful substances within the system compared to other configurations.

Moreover, the PEI leaving the system, expressed as a mass per unit of product stream, for the toxicological category. In this case, it was found that the ATP category's contribution is insignificant compared to the other impact categories. Therefore, a

commercial installation of these processes could be located near aquatic ecosystems without causing environmental problems for the ecosystems.

The rice husk process yields the highest PEI production rates. HTPI and TTP are the categories that contribute the largest proportion to the output PEI, with a value of 0.0532 PEI/kg in the vapor scenario for each biomass. This result indicates that the plants for this process should be in an ecologically resistant area, without contact with animals or vegetation. However, it is worth noting that these values remained low for this type of processing, confirming the favorable environmental performance of both scenarios [50]. Furthermore, these two categories are closely related, as both are calculated based on the lethal dose per ingestion that would kill 50% of a sample of rats. When analyzing the components of the process, 33% of the components contribute to these impact categories (HTPI and TTP), with acrolein and furfural making the most significant contributions at 46 mg/kg and 65 mg/kg (normalized impact scores of 8.18 and 5.79, respectively).

On the other hand, the GWP and ODP values are insignificant in all cases, suggesting that these bioprocesses would not pose significant concerns for global atmospheric pollution over time. However, the PCOP category had the greatest impact, at 0.0112 PEI/kg, in the rice husk and steam scenario.

This impact is primarily associated with product streams that could accelerate photochemical smog formation in these systems. In turn, a value of 0.00578 PEI/kg (rice husk and steam scenario) was obtained in the AP category. This metric, associated with potential environmental acidification, could indicate that the process generates

moderate gas emissions into the atmosphere (compared to the other categories analyzed) that can later end up in soil and water bodies.

Table 2 summarizes the environmental impact produced within the system on a per-unit-of-product basis (PEI/kg product), considering both toxicological and atmospheric effects. The results indicate that the toxicological category exhibits both positive and negative generation rates depending on the operating conditions.

In the case of air gasification, negative values are observed for the HTPI and TTP indicators, which suggests a net reduction of environmental impact within the system. This behavior implies that the harmful effects associated with the incoming substances are lower than those of the streams leaving the process. In contrast, the steam-based scenarios show positive generation values of approximately 0.018 PEI/kg for the same categories, indicating the presence of additional impacts related to human and terrestrial toxicity.

Despite these differences, the magnitude of the generated impacts remains relatively low compared to values reported in similar studies [50] [51], confirming the overall favorable environmental performance of the evaluated processes.

3.2.2 Bio-crude gasification

Regarding PEI generation rates, this process yields excellent results, with negative magnitudes across all scenarios. In the case of rice husk, it obtained generation rates of -39.49 and -23.89 PEI/h as shown in Table 3. When the PEI out and the PEI generated have opposite values but are equal or nearly equal in magnitude, the process completely compensates for its emitted environmental impact with actions that counteract it,

achieving a net balance in environmental impact. This may reflect positive environmental practices and mitigation strategies implemented to reduce its environmental footprint and promote sustainability. Rice husk gasification with air obtained higher impact output rates in this case.

Analyzing the impact categories, we found that this process yielded values for the HTPI, HTPE, and TTP categories, which correspond to toxicological, and for the PCOP and AP categories, which correspond to atmospheric. In this case, all toxicological categories showed negative generation rates; this outcome indicated that this biorefinery could transform incoming raw materials into less harmful products to terrestrial and human health. In the HTPI category, it can be noted that the scenarios with EFB, both water and steam, exhibit output PEI rates of 0 and negative generation rates. This result indicates that, for each unit of mass of product generated, the process mitigates or absorbs negative environmental impacts of -0.0067 and -0.0126 units for air and steam, respectively.

Regarding the AP category, it can be observed that the EFBs do not exhibit output or PEI generation rates, indicating that this process is neutral with respect to these categories. In turn, in the atmospheric category, the PCOP presents the highest PEI output rates, 0.0144 and 0.0163 PEI/kg for EFB and rice husk, respectively, with the steam-gasification scenario contributing the most for biomass. This indicates that these processes are generating a significant amount of substances or compounds that have the potential to contribute to the formation of smog and other air quality problems,

highlighting the importance of taking measures to reduce this negative impact on air quality and environmental health.

The results obtained in this study highlight the potential of indirect biomass gasification routes, particularly those involving bio-oil and bio-crude, as promising pathways for syngas production. However, several aspects require further investigation to enhance the reliability and industrial applicability of these systems.

First, although the present work employed equilibrium-based modeling in Aspen Plus®, the literature reports bio-crude steam gasification experiments, both catalytic [52][53] and non-catalytic [54], [55]. Although biochar acts as both a carbon source and an in-situ catalyst, enhancing reactivity, syngas quality, and tar suppression [56]. Catalytic steam gasification experiments in fixed beds at the lab scale yield relatively high hydrogen yields of around 800 °C, with carbon conversion of 66-80% [57][23]. Steam gasification of bio-crude can also produce hydrogen-rich gas, and the high gas yields (especially for H_2 and CO) are obtained at around 900 °C [54].

In comparison, the results of this study, under similar high-temperature conditions, show trends in hydrogen-rich syngas production comparable to those observed under steam-based scenarios. However, the absence of explicit catalytic effects in the present Aspen Plus® simulations may explain the lower hydrogen yields observed relative to catalytic experimental studies. This highlights the potential role of biochar not only as an energy carrier in bio-crude formulations but also as a promoter of gasification reactions. Therefore, incorporating catalytic effects or more detailed reaction

mechanisms into the model could further improve the prediction of syngas composition and process performance.

Second, while steam gasification improves exergy efficiency, it also requires additional external energy input, revealing a clear trade-off between thermodynamic performance and process energy demand. Future optimization studies should focus on integrating heat recovery systems, process intensification strategies, or renewable heat sources to mitigate these energy penalties.

From an environmental perspective, the results indicate that feedstock selection plays a critical role in determining potential environmental impacts. Biomass with high ash content, such as rice husk, leads to higher PEI values due to increased solid residues and emissions. Therefore, future studies should evaluate pretreatment strategies or blending approaches to reduce ash-related impacts and improve overall sustainability.

Additionally, the use of the Waste Reduction Algorithm (WAR) provided valuable insights into process-level environmental performance. However, integrating WAR with life cycle assessment (LCA) methodologies would allow for a more comprehensive evaluation, capturing upstream and downstream impacts and enabling more robust sustainability comparisons.

Finally, this study supports the potential of bio-oil and bio-crude as intermediate energy carriers that enable the decoupling of biomass supply and syngas production. This opens opportunities for decentralized pyrolysis units coupled with centralized gasification facilities. Future research should explore the techno-economic feasibility and supply chain

implications of such configurations, particularly in regions with dispersed biomass resources.

Overall, advancing bio-crude gasification requires a multi-scale approach combining improved reaction modeling, process integration, and sustainability assessment to bridge the gap between simulation and industrial deployment.

4. CONCLUSIONS

This study developed a simulation framework in Aspen Plus® to evaluate the thermodynamic performance of bio-oil and bio-crude gasification pathways for syngas production using two different feedstocks: oil palm empty fruit bunches (EFB) and rice husk (RH). The results indicate that air gasification of EFB provides the highest energy efficiency (54.5%), along with a corresponding exergy efficiency of 64.1%. In contrast, systems based on rice husk exhibit lower performance due to their elevated ash content, with energy and exergy efficiencies of 43.03% and 54.4%, respectively.

For bio-crude gasification, EFB achieves energy efficiencies of 50.7% and 44.3% under air and steam conditions, respectively, whereas rice husk reaches 41.1% and 37.6% under the same operating conditions. Overall, the use of steam as a gasifying agent enhances exergy efficiency for both feedstocks, although this advantage is accompanied by an increase in energy demand.

From an environmental perspective, higher potential environmental impacts (PEI) are associated with bio-oil gasification, particularly when rice husk is used as feedstock. The maximum PEI values were observed for steam-based operation with rice husk, reaching 61.1 PEI/h. This behavior is mainly attributed to the higher ash content and the

generation of additional pollutants during the conversion process. Future research should focus on integrating broader sustainability criteria, including safety, health considerations, and process uncertainty, to support more comprehensive decision-making.

Overall, the results indicate that indirect gasification pathways based on bio-oil and bio-crude can offer performance comparable to that of direct biomass gasification, particularly when low-ash feedstocks are used. However, the identified trade-offs between energy efficiency, exergy performance, and environmental impacts highlight the need for integrated process optimization strategies. These findings suggest that feedstock selection and process configuration are critical design variables for developing efficient and sustainable biorefineries.

ACKNOWLEDGMENT

Ana Buelvas thanks to Minciencias through the 2019 Bicentennial National Doctoral Scholarships, contracts UN-OJ-2020-47414. A special acknowledgment to Universidad del Norte and Universidad Tecnológica de Bolivar for supplied support.

651 **NOMENCLATURE**
652

EFB	Empty Fruit Bunches
RH	Rice Husk
HHV	Higher Heating Value, kJ/kg
LCA	Life Cycle Assessment
Qdry	Heat demanded by the drying section [kW]
Qncg	Heat demanded by combustion of NCG [kW]
Qcomb	Heat demanded by combustion of biohcar[kW]
W	Input power [kW]
$\dot{m}$	Mass flow [kg/h]
η_T	Energy efficiency
η_{Ex}	Exergy efficiency
$\dot{E}$	Energy flow rate [kW]
$\dot{X}$	Total exergy [kW]
$\dot{X}_{ph}$	Physical exergy [kW]
$\dot{X}_{ch}$	Chemical exergy [kW]
$Cp_{biochar}$	Specific heat capacity of biochar [kJ/kg K]
$\dot{X}_{ph_{biochar}}$	Physical exergy of biochar [kW]
x_i^{ch}	Standard chemical exergy of component i.
h	Enthalpy [kJ/kg]
s	Entropy [kJ/kg K]

T_0	Temperature in the dead state (298.15 K and 101.325 kPa) [°C]
s_0	Enthalpy in the dead state (298.15 K and 101.325 kPa) [kJ/kg]
h_0	Entropy in the dead state (298.15 K and 101.325 kPa) [kJ/kg]
x_i	Molar fraction of component i
$\dot{n}$	Molar flow rate, mol/s or mol/h?
NCG	Non-condensable-Gases
WAR	Waste Reduction Algorithm
PEI	Potential environmental impact
ATP	Potential aquatic toxicity
HTPI	Human toxicity potential by ingestion
TTP	Terrestrial toxicity potential
HTPE	Human toxicity potential by inhalation or dermal exposure
ODP	Ozone depletion potential
GWP	Global warming potential
PCOP	Photochemical oxidation potential
PTX	
W	Intlet Work [kW]
R	Universal gas constant, kJ/kmol K
AP	Acidification potential
$i_{we}^{(cp)}$	Rate of PEI out of the system because of the release of waste energy due to chemical processes
$i_{out}^{(cp)}$	Rate of PEI leaving the system due to chemical interactions

$i_{out}^{(ep)}$	Rate of PEI out of the system due to energy generation processes
$i_{we}^{(ep)}$	Rate of PEI out of the system because of the release of waste energy due to energy generation
$i_{in}^{(cp)}$	Input rate of PEI to the chemical process
$i_{in}^{(ep)}$	input rate of PEI to the energy generation process

653
654

REFERENCES

[1] M. Carus, L. Dammer, A. Raschka, P. Skoczinski, and C. Vom Berg, "Renewable Carbon – Key to a Sustainable and Future-Oriented Chemical and Plastic Industry," 2020. [Online]. Available: www.bio-based.eu/nova-papers

[2] G. Kyriakarakos, C. Lindeque, and N. Shaffudah, "Development of a Sustainable Carbon Carrier for PtX Use: From Namibia to a Global Market.," 2023. [Online]. Available: www.ptx-hub.org

[3] A. Gonzalez-Quiroga *et al.*, "Design and cold flow testing of a Gas-Solid Vortex Reactor demonstration unit for biomass fast pyrolysis," *Chemical Engineering Journal*, vol. 329, pp. 198–210, Dec. 2017, doi: 10.1016/j.cej.2017.06.003.

[4] N. Dahmen, E. Henrich, E. Dinjus, and F. Weirich, "The bioliq® bioslurry gasification process for the production of biosynfuels, organic chemicals, and energy," *Energy Sustain. Soc.*, vol. 2, no. 1, pp. 1–44, 2012, doi: 10.1186/2192-0567-2-3.

[5] H. Chen *et al.*, "A review on bioslurry fuels derived from bio-oil and biochar: Preparation, fuel properties and application," Jan. 01, 2024, *Elsevier Ltd*. doi: 10.1016/j.fuel.2023.129283.

[6] Y. Gao *et al.*, "Syngas Production from Biomass Gasification: Influences of Feedstock Properties, Reactor Type, and Reaction Parameters," *ACS Omega*, vol. 8, no. 35, pp. 31620–31631, 2023, doi: 10.1021/acsomega.3c03050.

[7] M. Cortazar *et al.*, "Syngas production by bio-oil steam gasification in a fountain confined conical spouted bed reactor," *Fuel*, vol. 345, p. 128228, 2023, doi: 10.1016/j.fuel.2023.128228.

[8] H. Ishaq, S. Islam, I. Dincer, and B. S. Yilbas, "Development and performance investigation of a biomass gasification based integrated system with thermoelectric generators," *J. Clean. Prod.*, vol. 256, p. 120625, 2020, doi: https://doi.org/10.1016/j.jclepro.2020.120625.

[9] S. Zhang, N. Gao, C. Quan, F. Wang, and C. Wu, "Autothermal CaO looping biomass gasification to increase process energy efficiency and reduce ash sintering," *Fuel*, vol. 277, p. 118199, 2020, doi: 10.1016/j.fuel.2020.118199.

[10] H. Wu, Q. Liu, Z. Bai, G. Xie, J. Zheng, and B. Su, "Thermodynamics analysis of a novel steam/air biomass gasification combined cooling, heating and power system with solar energy," *Appl. Therm. Eng.*, vol. 164, p. 114494, 2020, doi: 10.1016/j.applthermaleng.2019.114494.

[11] A. Buelvas *et al.*, "Gasification of solid biomass or fast pyrolysis bio-oil: Comparative energy and exergy analyses using AspenPlus®," *Engineering Reports*, vol. 6, no. 7, pp. 1–19, 2024, doi: 10.1002/eng2.12825.

[12] Q. Li, Y. Zhang, and G. Hu, "Techno-economic analysis of advanced biofuel production based on bio-oil gasification," *Bioresour. Technol.*, vol. 191, pp. 88–96, 2015, doi: 10.1016/j.biortech.2015.05.002.

[13] R. M. Swanson, A. Platon, J. A. Satrio, and R. C. Brown, "Techno-economic analysis of biomass-to-liquids production based on gasification," *Fuel*, vol. 89, no. SUPPL. 1, pp. S11–S19, 2010, doi: 10.1016/j.fuel.2010.07.027.

[14] J. L. Zheng, Y. H. Zhu, M. Q. Zhu, H. T. Wu, and R. C. Sun, "Bio-oil gasification using air - Steam as gasifying agents in an entrained flow gasifier," *Energy*, vol. 142, pp. 426–435, 2018, doi: 10.1016/j.energy.2017.10.031.

[15] P. Feng, X. Li, J. Wang, J. Li, H. Wang, and L. He, "The mixtures of bio-oil derived from different biomass and coal/char as biofuels: Combustion characteristics," *Energy*, vol. 224, 2021, doi: 10.1016/j.energy.2021.120132.

[16] B. Alonso-Fariñas, A. Gallego-Schmid, P. Haro, and A. Azapagic, "Environmental assessment of thermo-chemical processes for bio-ethylene production in comparison with bio-chemical and fossil-based ethylene," *J. Clean. Prod.*, vol. 202, pp. 817–829, 2018, doi: https://doi.org/10.1016/j.jclepro.2018.08.147.

[17] J. Bare, "TRACI 2.0: the tool for the reduction and assessment of chemical and other environmental impacts 2.0," *Clean Technol. Environ. Policy*, vol. 13, no. 5, pp. 687–696, 2011, doi: 10.1007/s10098-010-0338-9.

[18] D. M. Young and H. Cabezas, "Designing sustainable processes with simulation: the waste reduction (WAR) algorithm," *Comput. Chem. Eng.*, vol. 23, no. 10, pp. 1477–1491, 1999, doi: https://doi.org/10.1016/S0098-1354(99)00306-3.

[19] M.-O. P. Fortier, G. W. Roberts, S. M. Stagg-Williams, and B. S. M. Sturm, "Life cycle assessment of bio-jet fuel from hydrothermal liquefaction of microalgae," *Appl. Energy*, vol. 122, pp. 73–82, 2014, doi: https://doi.org/10.1016/j.apenergy.2014.01.077.

[20] E. Ranzi, P. E. A. Debiagi, and A. Frassoldati, "Mathematical Modeling of Fast Biomass Pyrolysis and Bio-Oil Formation. Note I: Kinetic Mechanism of Biomass Pyrolysis," *ACS Sustain. Chem. Eng.*, vol. 5, no. 4, pp. 2867–2881, 2017, doi: 10.1021/acssuschemeng.6b03096.

[21] M. B. Gorensek, R. Shukre, and C. C. Chen, "Development of a Thermophysical Properties Model for Flowsheet Simulation of Biomass Pyrolysis Processes," *ACS Sustain. Chem. Eng.*, vol. 7, no. 9, pp. 9017–9027, 2019, doi: 10.1021/acssuschemeng.9b01278.

[22] A. Buelvas *et al.*, "Gasification of solid biomass or fast pyrolysis bio-oil: Comparative energy and exergy analyses using AspenPlus®," *Engineering Reports*, vol. 6, no. 7, Jul. 2024, doi: 10.1002/eng2.12825.

[23] H. Chen *et al.*, "A review on bioslurry fuels derived from bio-oil and biochar: Preparation, fuel properties and application," Jan. 01, 2024, *Elsevier Ltd*. doi: 10.1016/j.fuel.2023.129283.

[24] E. Henrich, F. Weirich, F. Karlsruhe, and F. Karlsruhe, "Pressurized Entrained Flow Gasifiers for Biomass," 2004.

[25] D. Katla-Milewska, S. M. Nazir, and A. Skorek-Osikowska, "Synthetic natural gas (SNG) production with higher carbon recovery from biomass: Techno-economic assessment," *Energy Convers. Manag.*, vol. 300, Jan. 2024, doi: 10.1016/j.enconman.2023.117895.

[26] P. Nathrath, F. Kroll, D. Karmann, M. Geißelbrecht, and P. Schühle, "Methanol production in a sustainable, mild and competitive process: concept launch and analysis," *Green Chemistry*, vol. 27, no. 30, pp. 9268–9279, Jul. 2025, doi: 10.1039/d5gc01307k.

[27] W. Chan, T. Morosuk, X. Li, and H. Li, "Exergoeconomic Analysis and Tri-Objective Optimization of the Allam Cycle Co-Fired by Biomass and Natural Gas," *Journal of Energy Resources Technology, Transactions of the ASME*, vol. 145, no. 12, 2023, doi: 10.1115/1.4062528.

[28] M. Wądrzyk, R. Janus, Ł. Korzeniowski, and M. Plata, "Thermochemical Co-Liquefaction of Fruit Pomace's Blends in a Binary Solvent System Toward Value-Added Bioproducts," *Journal of Energy Resources Technology, Transactions of the ASME*, vol. 146, no. 3, 2024, doi: 10.1115/1.4064357.

[29] H. Ishaq and I. Dincer, "An Efficient Energy Utilization of Biomass Energy-Based System for Renewable Hydrogen Production and Storage," *Journal of Energy Resources Technology, Transactions of the ASME*, vol. 144, no. 1, 2022, doi: 10.1115/1.4050875.

[30] K. R. G. Burra, M. Sahin, Y. Zheng, and A. K. Gupta, "Near-Critical CO2-Assisted Liquefaction-Extraction of Biomass and Wastes to Fuels and Value-Added Products," *Journal of Energy Resources Technology, Transactions of the ASME*, vol. 146, no. 1, 2024, doi: 10.1115/1.4063813.

[31] Z. Wang *et al.*, "Products Distribution and Synergistic Effects Analysis During Co-Pyrolysis of Agricultural Residues and Waste Tire Using Gas Chromatography/ Mass Spectrometry," *J. Energy Resour. Technol.*, vol. 145, no. 8, 2023, doi: 10.1115/1.4056940.

[32] W. J. Liu and H. Q. Yu, "Thermochemical Conversion of Lignocellulosic Biomass into Mass-Producible Fuels: Emerging Technology Progress and Environmental Sustainability Evaluation," *ACS Environmental Au*, vol. 2, no. 2, pp. 98–114, 2022, doi: 10.1021/acsenvironau.1c00025.

[33] K. I. M. Al-Malah, "Flash Separation and Distillation Columns," in *Aspen Plus®:Chemical Engineering Applications*, John Wiley & Sons, Ltd, 2016, ch. 4, pp. 99–129. doi: 10.1002/9781119293644.ch4.

[34] J. Purkaystha, S. Prasher, M. T. Afzal, C. Nzediegwu, and J. Dhiman, "Wheat straw biochar amendment significantly reduces nutrient leaching and increases green pepper yield in a less fertile soil," *Environ. Technol. Innov.*, vol. 28, p. 102655, 2022, doi: 10.1016/j.eti.2022.102655.

[35] H. Lu *et al.*, "Effects of biochar on soil microbial community and functional genes of a landfill cover three years after ecological restoration," *Science of the Total Environment*, vol. 717, p. 137133, 2020, doi: 10.1016/j.scitotenv.2020.137133.

[36] S. Rawat, C. T. Wang, C. H. Lay, S. Hotha, and T. Bhaskar, "Sustainable biochar for advanced electrochemical/energy storage applications," *J. Energy Storage*, vol. 63, no. March, p. 107115, 2023, doi: 10.1016/j.est.2023.107115.

[37] J. F. Peters, F. Petrakopoulou, and J. Dufour, "Exergetic analysis of a fast pyrolysis process for bio-oil production," *Fuel Processing Technology*, vol. 119, pp. 245–255, 2014, doi: 10.1016/j.fuproc.2013.11.007.

[38] T. J. Kotas, Ed., "Appendix A - Chemical exergy and enthalpy of devaluation," in *The Exergy Method of Thermal Plant Analysis*, Butterworth-Heinemann, 1985, pp. 236–262. doi: https://doi.org/10.1016/B978-0-408-01350-5.50014-3.

[39] D. R. Morris and J. Szargut, “Standard chemical exergy of some elements and compounds on the planet earth,” *Energy*, vol. 11, no. 8, pp. 733–755, 1986, doi: https://doi.org/10.1016/0360-5442(86)90013-7.

[40] G. Song, L. Shen, and J. Xiao, “Estimating specific chemical exergy of biomass from basic analysis data,” *Ind. Eng. Chem. Res.*, vol. 50, no. 16, pp. 9758–9766, 2011, doi: 10.1021/ie200534n.

[41] M. G. "Groenli, “A theoretical and experimental study of the thermal degradation of biomass,” Norway, 1996. doi: https://doi.org/.

[42] D. M. Young and H. Cabezas, “Designing sustainable processes with simulation: the waste reduction (WAR) algorithm,” 1999. [Online]. Available: www.elsevier.com/locate/compchemeng

[43] S. I. Meramo-Hurtado, P. Puello, and J. Rodríguez, “Computer-aided environmental assessment applied for estimation of ecological impacts derived from topological pathways based on lignocellulosic biomass transformation,” *Applied Sciences (Switzerland)*, vol. 10, no. 18, Sep. 2020, doi: 10.3390/APP10186586.

[44] D. Young, R. Scharp, and H. Cabezas, “The waste reduction (WAR) algorithm: environmental impacts, energy consumption, and engineering economics,” 2000. [Online]. Available: www.elsevier.nl/locate/wasman

[45] K. Moreno-Sader, S. I. Meramo-Hurtado, and A. D. González-Delgado, “Computer-aided environmental and exergy analysis as decision-making tools for selecting bio-oil feedstocks,” *Renewable and Sustainable Energy Reviews*, vol. 112, pp. 42–57, Sep. 2019, doi: 10.1016/j.rser.2019.05.044.

[46] K. Moreno-Sader, S. I. Meramo-Hurtado, and A. D. González-Delgado, “Computer-aided environmental and exergy analysis as decision-making tools for selecting bio-oil feedstocks,” *Renewable and Sustainable Energy Reviews*, vol. 112, pp. 42–57, 2019, doi: 10.1016/j.rser.2019.05.044.

[47] S. J. Arteaga-Díaz, S. I. Meramo-Hurtado, J. León-Pulido, A. Zuorro, and A. D. González-Delgado, “Environmental Assessment of Large Scale Production of Magnetite (Fe3O4) Nanoparticles via Coprecipitation,” *Applied Sciences*, vol. 9, no. 8, 2019, doi: 10.3390/app9081682.

[48] J. L. Zheng, Y. H. Zhu, M. Q. Zhu, H. T. Wu, and R. C. Sun, “Bio-oil gasification using air - Steam as gasifying agents in an entrained flow gasifier,” *Energy*, vol. 142, pp. 426–435, 2018, doi: 10.1016/j.energy.2017.10.031.

[49] H. Guo, F. Peng, H. Zhang, and L. Xiong, “Production of hydrogen rich bio-oil derived syngas from co-gasification of bio-oil and waste engine oil as feedstock for lower alcohols synthesis in two-stage bed reactor,” *Int. J. Hydrogen Energy*, vol. 39, no. 17, pp. 9200–9211, 2014, doi: 10.1016/j.ijhydene.2014.04.008.

[50] S. I. Meramo-Hurtado, P. Puello, and J. Rodríguez, “Computer-aided environmental assessment applied for estimation of ecological impacts derived from topological pathways based on lignocellulosic biomass transformation,” *Applied Sciences (Switzerland)*, vol. 10, no. 18, pp. 1–26, 2020, doi: 10.3390/APP10186586.

[51] A. Vargas-Mira, C. Zuluaga-García, and Á. D. González-Delgado, “A Technical and Environmental Evaluation of Six Routes for Industrial Hydrogen Production from

Empty Palm Fruit Bunches," *ACS Omega*, vol. 4, no. 13, pp. 15457–15470, Sep. 2019, doi: 10.1021/acsomega.9b01683.

[52] J. Yao *et al.*, "Biomass to hydrogen-rich syngas via steam gasification of bio-oil/biochar slurry over LaCo1-xCuxO3 perovskite-type catalysts," *Energy Convers. Manag.*, vol. 117, pp. 343–350, Jun. 2016, doi: 10.1016/j.enconman.2016.03.043.

[53] G. Chen, J. Yao, J. Liu, B. Yan, and R. Shan, "Biomass to hydrogen-rich syngas via catalytic steam gasification of bio-oil/biochar slurry," *Bioresour. Technol.*, vol. 198, pp. 108–114, 2015, doi: 10.1016/j.biortech.2015.09.009.

[54] H. Sui *et al.*, "Integrated study on gasification of bio-slurry: Experimental validation and computational modeling," *Journal of the Energy Institute*, vol. 125, Apr. 2026, doi: 10.1016/j.joei.2026.102457.

[55] H. Sui, X. Wang, and H. Chen, "Rheological Behavior and Steam Gasification of Bio-slurry," in *Energy Procedia*, Elsevier Ltd, 2015, pp. 220–225. doi: 10.1016/j.egypro.2015.07.310.

[56] W. Mo *et al.*, "Gasification mechanism of biomass bio-slurry based on a novel photothermal fluidized bed thermogravimetric analysis," *J. Environ. Manage.*, vol. 398, Jan. 2026, doi: 10.1016/j.jenvman.2025.128399.

[57] J. Yao *et al.*, "Biomass to hydrogen-rich syngas via steam gasification of bio-oil/biochar slurry over LaCo1-xCuxO3 perovskite-type catalysts," *Energy Convers. Manag.*, vol. 117, pp. 343–350, 2016, doi: 10.1016/j.enconman.2016.03.043.

[58] Phyllis, "Phyllis Data Base." Accessed: Oct. 23, 2025. [Online]. Available: https://phyllis.nl/Browse/Standard/ECN-Phyllis

Figure Captions List

Fig 1. Schematic diagram of the simulation of the fast pyrolysis process. In this Fig, Qdry, Qncg, and Qcomb mean the heat demanded by the drying section and the heat supplied by the combustion of NCG and biochar, respectively.

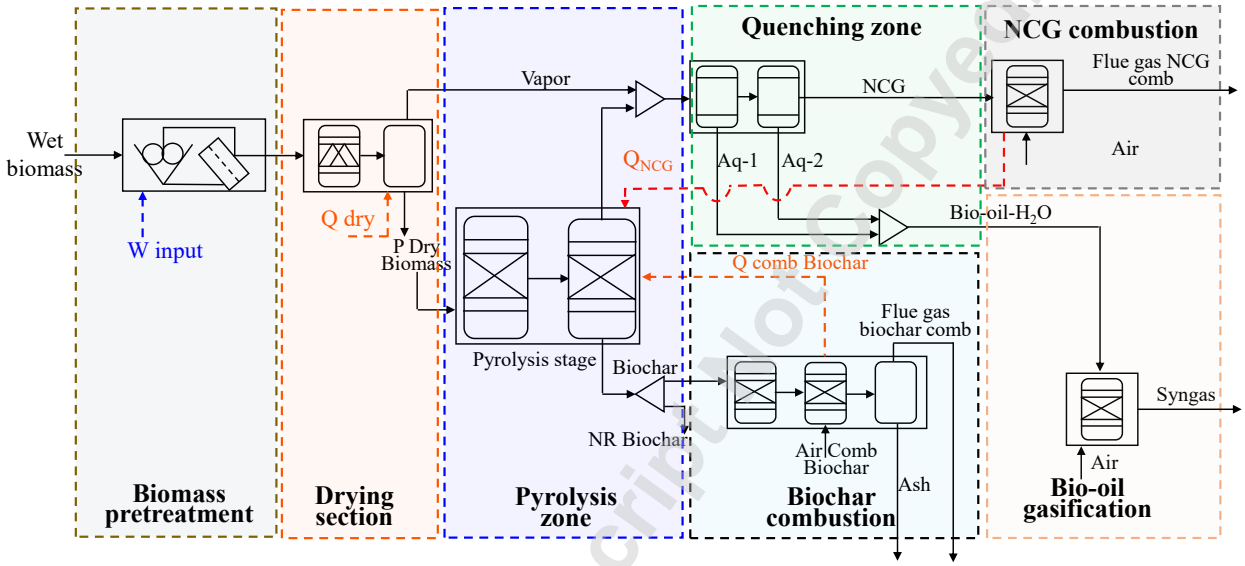

875 Fig 2. Schematic diagram summarizing the main streams used for energy and exergy
876 calculations. Airbio-oil changes to airbio-crude, steambio-oil, or steambio-crude, as
877 applicable to the gasification scenario evaluated.

878

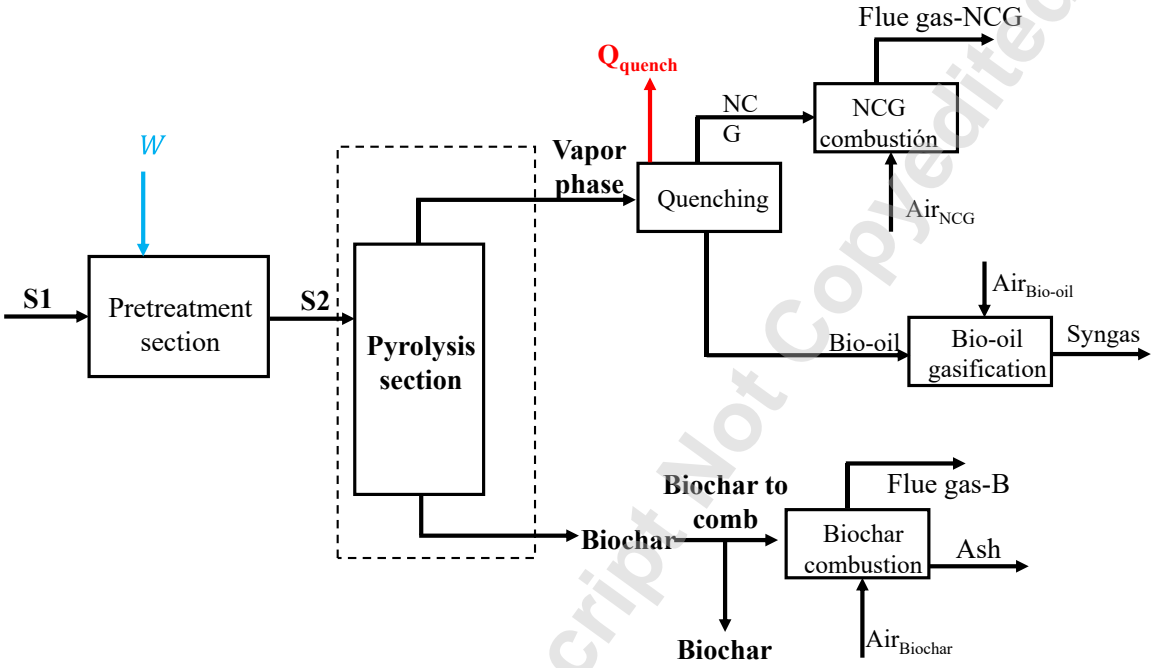

879
880

Fig 3. Sankey diagrams for the fast pyrolysis-bio-oil gasification of empty fruit bunches a) using air and b) using steam as gasification agent. Corresponding Grassmann diagrams c) using air and d) using steam as gasification agent.

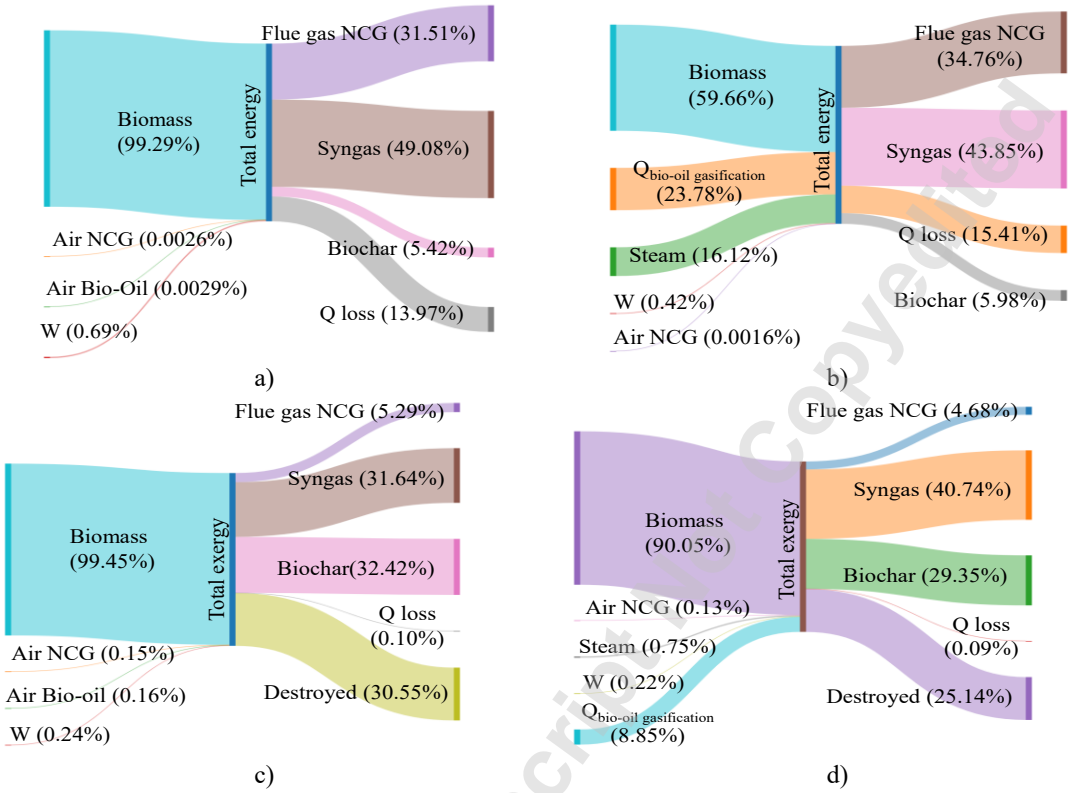

Fig 4. Sankey diagrams for the fast pyrolysis and bio-oil gasification for rice husk. a) using air as gasification agent. b) using steam as gasification agent. Grassmann diagrams for fast pyrolysis and bio-oil gasification. c) using air as gasification agent. d) using steam as gasification agent.

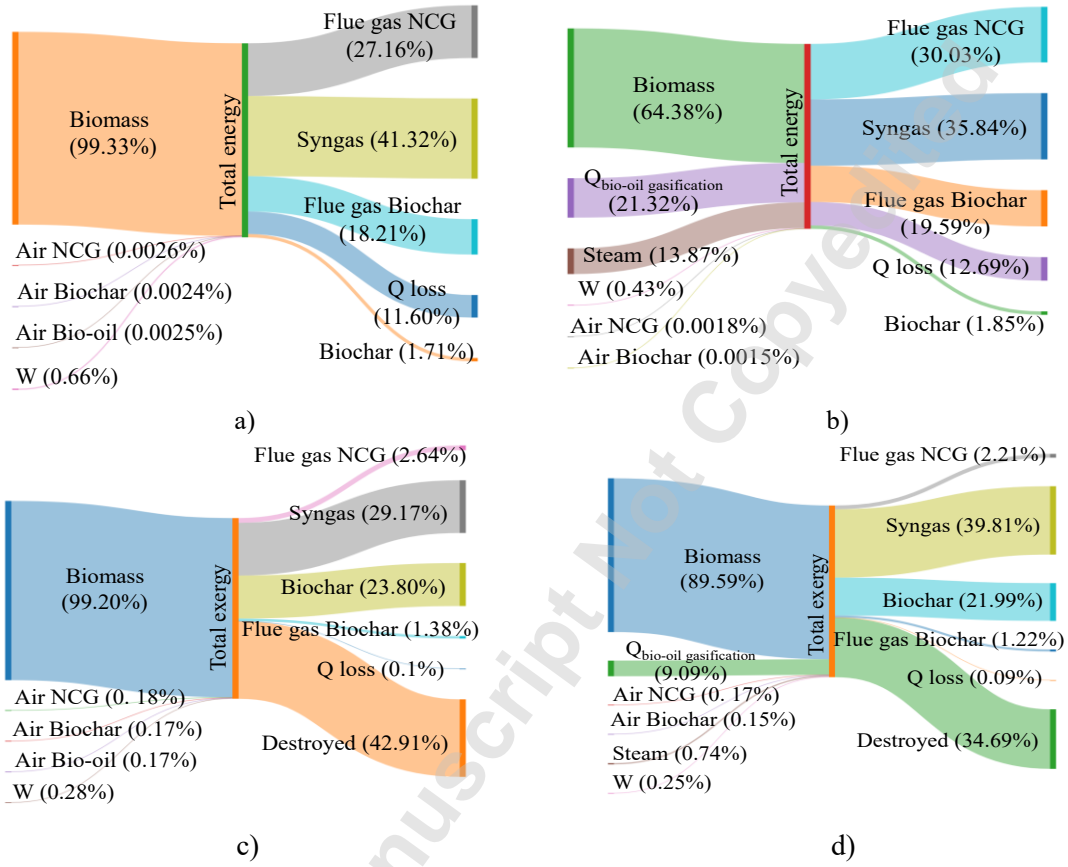

Fig 5. Grassmann diagrams for EFB the fast pyrolysis and bio-crude gasification. a) results for rice husk using air as the gasification agent. b) results for rice husk using steam as gasification agent. c) results for rice husk using air as gasification agent. d) results for rice husk using steam as gasification agent.

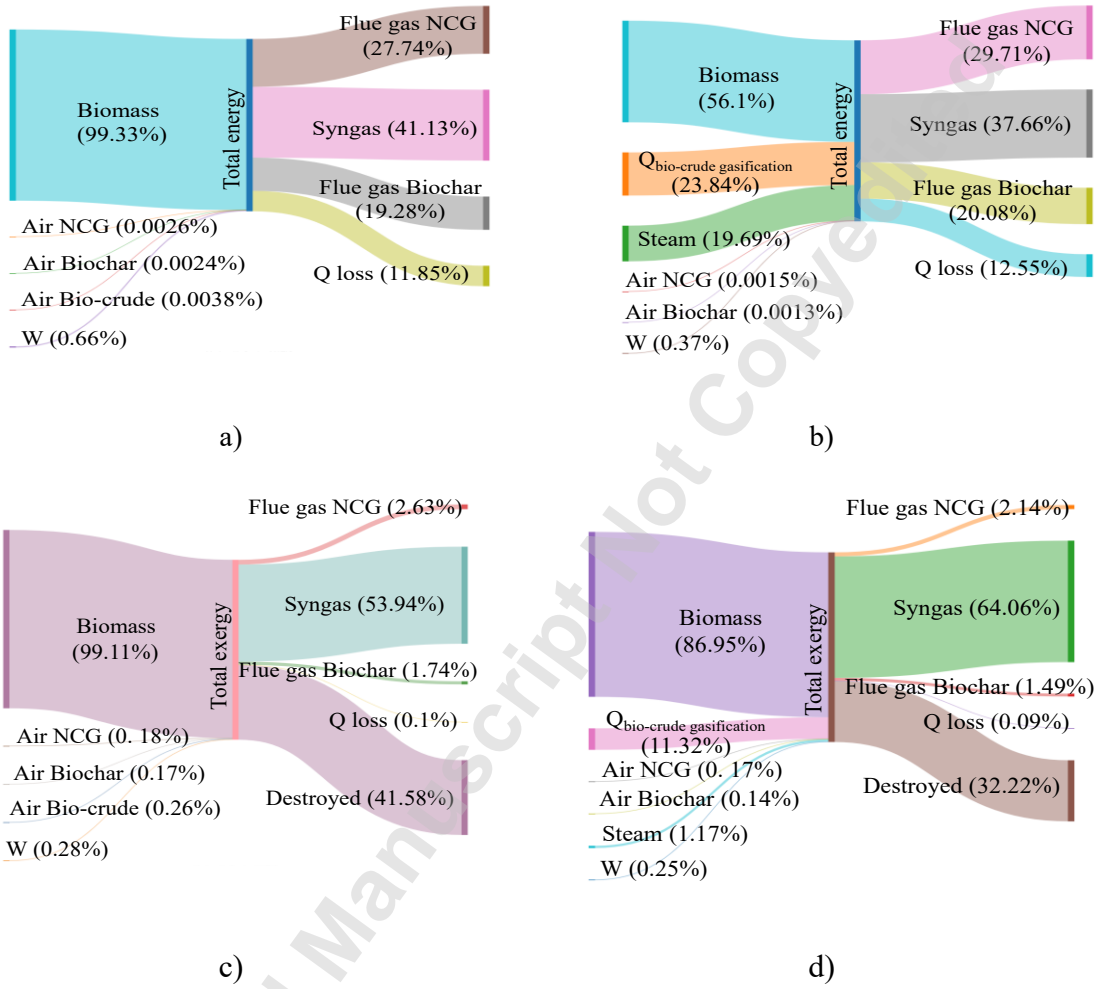

Fig 6. Grassmann diagrams for RH fast pyrolysis and bio-crude gasification. A) results for EFB using air as the gasification agent. B) results for EFB using steam as gasification agent. C) results for EFB using air as gasification agent. D) results for EFB using steam as gasification agent.

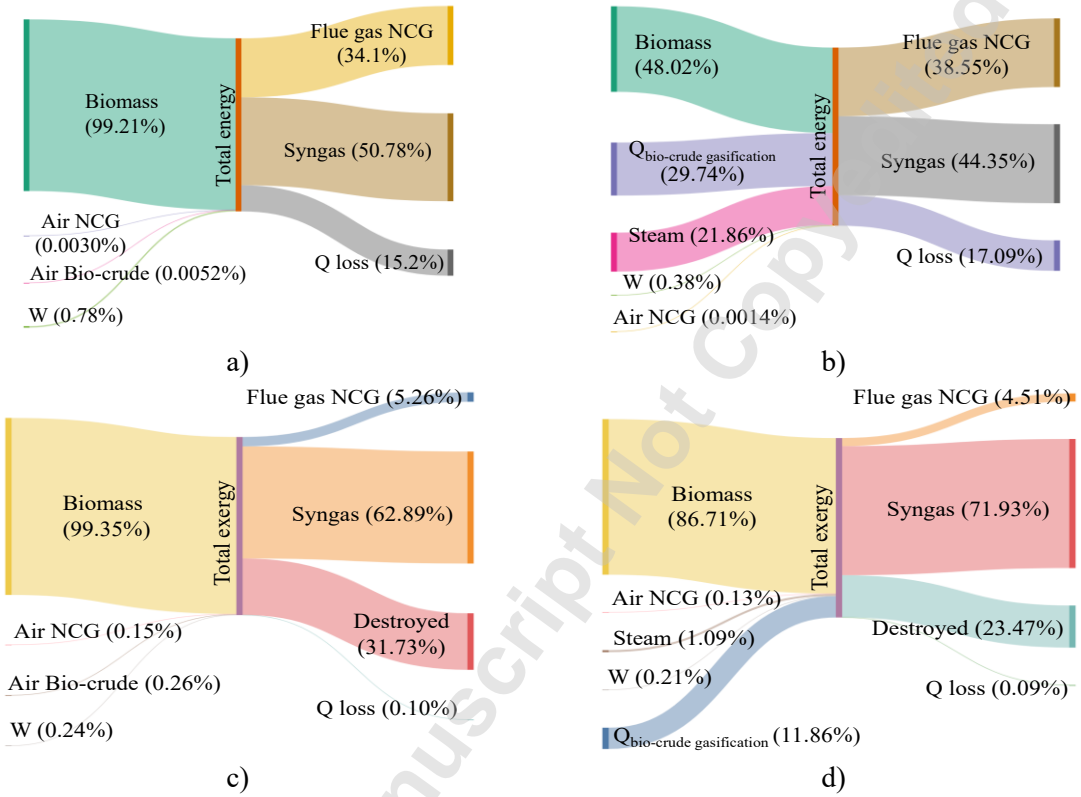

966 **Table Caption List**

967 Table 1. Ultimate and proximate analysis on a dry basis (db) and higher heating value

968 (HHV) of the feedstock. Ultimate analysis adapted from the Phyllis database [58] .

Analysis/parameter	Rice husk, RH	Empty fruit bunches, EFB
ULTANAL	**%wt, db**	**%wt, db**
C	39.3	45.7
H	4.7	5.5
N	0.0	0.0
Cl	0.0	0.0
S	0.0	0.0
O	35.9	43.5
PROXANAl	**%wt, db**	
Volatile matter, VM	60.0	71.1
Fixed carbon, FC	20.0	23.7
Ash, %wt db	20.0	5.1

969
970
971
972
973
974
975
976
977
978
979
980

Table 2. Global environmental impacts of the bio-oil gasification process using air and steam.

Condition	Oxidizing agent	Empty Fruit Bunch		Rice Husk	
		PEI/h	PEI/kg	PEI/h	PEI/kg
Iout	Air	25	0.033	88	0.08
	Steam	39	0.078	61	0.135
Igen	Air	3	0.002	9	0.004
	Steam	24	0.048	11	0.023

Category	Oxidizing agent	Empty Fruit Bunch		Rice Husk	
		PEI/h	PEI/kg	PEI/h	PEI/kg
HTPI	Air	0.007	-0.001	0.032	-0.002
	Steam	0.03	0.018	0.053	0
HTPE	Air	0.002	0.005	0.006	0
	Steam	0.012	0.005	0.007	0.002
TTP	Air	0.007	-0.001	0.032	-0.002
	Steam	0.03	0.018	0.053	0
PCOP	Air	0.002	0.003	0.005	0.005
	Steam	0.006	0.007	0.011	0.011
AP	Air	0	0	0.003	0.003
	Steam	0	0	0.006	0.006

Table 3. Global environmental impacts of the bio-crude gasification process using air and steam

1005

Condition	Oxidizing agent	Empty Fruit Bunch		Rice Husk	
		PEI/h	PEI/kg	PEI/h	PEI/kg
Iout	Air	25	0.03	88	0.08
	Steam	40	0.08	62	0.135
Igen	Air	3	0.002	6	0.004
	Steam	23	0.05	9	0.02

Category	Oxidizing agent	Empty Fruit Bunch		Rice Husk	
		PEI/h	PEI/kg	PEI/h	PEI/kg
HTPI	Air	0.008	-0.002	0.032	-0.003
	Steam	0.03	0.018	0.053	0
HTPE	Air	0.003	0.001	0.007	0.001
	Steam	0.012	0.005	0.008	0.002
TTP	Air	0.008	-0.002	0.032	-0.002
	Steam	0.031	0.018	0.053	0
PCOP	Air	0.004	0.003	0.006	0.005
	Steam	0.007	0.007	0.011	0.011
AP	Air	0.002	0.002	0.004	0.003
	Steam	0.003	0.003	0.006	0.006

1006
1007